Journal of Experimental Botany, Vol. 61, No. 4, pp. 1031–1039, 2010
doi:10.1093/jxb/erp368 Advance Access publication 15 December, 2009
This paper is available online free of all access charges (see http://jxb.oxfordjournals.org/open_access.html for further details)

Journal of Experimental Botany
www.jxb.oxfordjournals.org

RESEARCH PAPER

Photosynthesis in lightfleck areas of homobaric and heterobaric leaves

Roland Pieruschka[1,2,*], Andrés Chavarría-Krauser[3], Ulrich Schurr[1] and Siegfried Jahnke[1,4]

[1] ICG-3: Phytosphere, Forschungszentrum Jülich, D-52425 Jülich, Germany
[2] Department of Global Ecology, Carnegie Institution of Washington, Stanford, CA 94305, USA
[3] Institute of Applied Mathematics, Universität Heidelberg, D-69120 Heidelberg, Germany
[4] FB Biologie und Geographie, Universität Duisburg-Essen, D-45117 Essen, Germany

* To whom correspondence should be addressed. E-mail: r.pieruschka@fz-juelich.de

Received 5 June 2009; Revised 23 November 2009; Accepted 24 November 2009

Abstract

Leaves within a canopy are exposed to a spatially and temporally fluctuating light environment which may cause lateral gradients in leaf internal CO_2 concentration and diffusion between shaded and illuminated areas. In previous studies it was hypothesized that lateral CO_2 diffusion may support leaf photosynthesis, but the magnitude of this effect is still not well understood. In the present study homobaric leaves of *Vicia faba* or heterobaric leaves of *Glycine max* were illuminated with lightflecks of different sizes, mimicking sunflecks. Photosynthetic properties of the lightfleck areas were assessed with combined gas exchange measurements and chlorophyll fluorescence imaging. Lateral diffusion in homobaric leaves with an interconnected intercellular air space stimulated photosynthesis and the effect was largest in small lightfleck areas, in particular when plants were under drought stress. Such effects were not observed in the heterobaric leaves with strongly compartmented intercellular gas spaces. It is concluded that lateral diffusion may significantly contribute to photosynthesis of lightfleck areas of homobaric leaves depending on lightfleck size, lateral diffusivity, and stomatal conductance. Since homobaric leaf structures have been reported for many plant species, it is hypothesized that leaf homobary may have an impact on overall plant performance under conditions with a highly heterogeneous light environment.

Key words: Drought stress, heterobaric leaves, homobaric leaves, lateral CO_2 diffusion, photosynthesis, sunflecks.

Introduction

Leaf photosynthesis is supplied with CO_2 mainly from ambient air (Hetherington and Woodward, 2003) or, to a minor degree, mitochondrial respiration (Loreto *et al.*, 2001; Pinelli and Loreto, 2003), but illuminated parts of leaf blades may also benefit from CO_2 diffusing from nearby shaded areas through intercellular air spaces which may be effective over a distance of several millimetres (Pieruschka *et al.*, 2006). The potential to use laterally diffusing CO_2 for photosynthesis depends on leaf anatomy. In heterobaric leaves, bundle sheath extensions provide internal barriers for gas diffusion, whereas homobaric leaves lack such extensions and have interconnected gas spaces open for lateral (peridermal) gas movement (Neger, 1918).

A lateral gradient in CO_2 concentration of homobaric leaves of *Commelina communis* was studied by using chlorophyll fluorescence imaging and was reported to affect photosynthetic CO_2 uptake over a distance of only 0.3 mm along the diffusion path (Morison *et al.*, 2005). For homobaric leaves of *Nicotiana tabacum* and *Vicia faba*, however, lateral CO_2 diffusion from shaded to illuminated leaf parts affected photosynthesis over distances up to 3–4 mm when stomatal conductance was low, for example in drought-stressed plants; this impact of lateral CO_2 flux disappeared when stomata reopened after irrigation and ambient CO_2 became the main source of photosynthesis (Pieruschka *et al.*, 2006).

The possible influence of lateral diffusion on photosynthesis was recently investigated by artificially closing stomata with grease and thus creating lateral CO_2 gradients inside leaves (Morison *et al.*, 2007; Pieruschka *et al.*, 2008). Both studies concluded that lateral diffusion may support photosynthesis, but with contrasting results considering heterobaric and homobaric leaves. On the one hand, lateral CO_2 flux rates were found to be effective over a range of no more than 1 mm and to be similar for both heterobaric and homobaric species (Morison *et al.*, 2007). On the other hand, large differences in rates and distances of lateral CO_2 supply were reported (Pieruschka *et al.*, 2008) and the authors concluded that the extent of lateral diffusion depends largely on the diffusivity of the intercellular air space. These studies were performed with artificially greased stomata which makes the estimation of the impact of lateral CO_2 diffusion on photosynthesis under sunfleck conditions in the field difficult. Here sunflecks were simulated by illuminating leaves of *V. faba* (homobaric) and *Glycine max* (heterobaric) consecutively with large or small lightflecks. Simultaneous measurement of gas exchange of the whole leaves and chlorophyll fluorescence imaging of the illuminated leaf areas were used to analyse net photosynthesis or quantum use efficiencies of lightfleck areas of plants exposed to progressive drought stress. The aim of the present work was to quantify the impact of lateral CO_2 diffusion (in addition to vertical gas diffusion through stomata) on photosynthetic carbon gain and light stress of lightfleck areas of homobaric and heterobaric leaves.

Materials and methods

Plant material and growth conditions

Plants of *G. max* (L.) Merr. cv. Williams (heterobaric leaves) and *V. faba* L. cv. Hangdown Grünkernig (homobaric) were grown from seeds in 1.0 l pots with soil (Einheitserde Typ ED; Balster Einheitserdewerk, Fröndenberg, Germany) in a greenhouse, periodically irrigated with tap water, and fertilized once a week. When the light intensity dropped below 110 μmol photons m^{-2} s^{-1}, artificial light was added (SON-T Agro, 400 W, Philips, Germany) providing a photosynthetic photon flux density (PPFD) of 400–450 μmol m^{-2} s^{-1} at 30 cm above the pots.

Gas exchange system and chlorophyll fluorescence measurements

Gas exchange of leaves was measured by an open gas exchange system (Jahnke, 2001). A leaf chamber was constructed to enclose whole leaves with a maximal area of 140 cm^2 kept in position by two nets made from nylon; the chamber bottom and the removable lid were covered with highly light-translucent teflon films (Nowofol EFEP-RP 5000, Kunststoffprodukte, Siegsdorf, Germany). The air provided to the leaf chamber was generated either by mixing CO_2-free air with gaseous CO_2 or by mixing N_2, O_2, and CO_2 with mass-flow controllers (F201; Bronkhorst-Mättig, Kamen, Germany); the CO_2 concentration of the incoming air was 350 μmol mol^{-1} in all experiments, whereas the O_2 concentration was 21% or 1%. The pressure difference between the atmosphere and the leaf chamber was kept at zero (Jahnke, 2001). Leaf temperature was 23–23.5 °C in darkness and 24–25 °C in the light. Net CO_2 exchange rates (*NCERs*; μmol CO_2 m^{-2} s^{-1}) and transpiration rates (*E*; mmol m^{-2} s^{-1}) were measured (Jahnke, 2001), and stomatal conductance for CO_2 (g_c) of the enclosed leaf was calculated (von Caemmerer and Farquhar, 1981). Chlorophyll fluorescence was detected with an Imaging-PAM Chlorophyll Fluorometer (Walz, Effeltrich, Germany). After plants were in darkness for 1 h, minimum (F_0) and maximum (F_m) fluorescence were recorded and used to calculate the quantum efficiency of dark-adapted leaves (F_v/F_m, with $F_v=F_m-F_0$). In actinic light (150 μmol photons m^{-2} s^{-1}), maximal fluorescence (F_m') and steady-state fluorescence prior to the flash (F) were measured while saturated light flashes were applied every 30 s. This was used to calculate the quantum efficiency of light-adapted leaves ($\Delta F/F_m'$, with $\Delta F=F_m'-F$). Electron transport rates ($ETR = \Delta F/F_m' \times PPFD \times 0.85 \times 0.5$; with 0.85 as an estimate of absorbed light and 0.5 accounting for the partitioning of light between photosystem I and II) and non-photochemical quenching ($NPQ=F_m/F'_m-1$) were calculated according to Genty *et al.* (1989) and Bilger and Björkman (1990), respectively.

Experimental protocols

Gas exchange and chlorophyll fluorescence were measured simultaneously on 24 (photorespiratory conditions) and 23 (non-photorespiratory conditions) attached *V. faba* leaves, and 22 (photorespiratory conditions) and 22 (non-photorespiratory conditions) *G. max* leaves. The plants were exposed to different drought stress levels from 1 d to 5 d without irrigation. The leaves were shaded by a template with a circular opening; the illuminated leaf area underneath was denoted as a large lightfleck area (LLF; Fig. 1C), with a diameter of 23 mm, a projected surface area of 4.15 cm^2, a perimeter of 7.2 cm, and a perimeter to area ratio of 1.7 cm^{-1}. A second template could be moved over the larger opening providing a small lightfleck (SLF; Fig. 1D), with a diameter of 10 mm, an area of 0.79 cm^2, a perimeter of 3.1 cm, and an perimeter to area ratio of 4.0 cm^{-1}. The ratio between the perimeter to area ratios of the LLF and SLF areas was 0.43.

The experiment started with the measurement of leaf respiration in the dark ($R_{leaf}=-NCER$). Then the leaf was illuminated with an LLF (Fig. 1C, F), and gas exchange rates of the whole leaf and chlorophyll fluorescence parameters of the LLF were measured for 8 min. Thereafter, the LLF lightfleck area was reduced to the SLF (Fig. 1D, G) and gas exchange rates of the whole leaf and chlorophyll fluorescence parameters of the SLF were measured for another 8 min.

Data analysis

Chlorophyll fluorescence parameters and gas exchange rates were measured for LLF and SLF at approximately steady-state conditions. Quantum efficiency of light-adapted leaves ($\Delta F/F_m'$), electron transport rate (*ETR*), and non-photochemical quenching (*NPQ*) were obtained for the LLF and SLF areas (Fig. 1). Gradients in $\Delta F/F_m'$ were measured on the images of SLF and LLF by averaging six linear transects; starting with a vertical transect and moving the following transects by 30° clockwise. The analysis was performed by using the free software Image J (http://rsbweb.nih.gov/ij/).

Stomatal conductance for CO_2 of the LLF area was calculated as:

$$g_{LLF} = g_{leaf,D} + (g_{leaf,LLF} - g_{leaf,D}) \frac{LA_{leaf}}{LA_{LLF}} \quad (1)$$

where $g_{leaf,D}$ is leaf conductance in darkness, $g_{leaf,LLF}$ is leaf conductance measured with illumination of LLF, LA_{leaf} is the area of the entire leaf, and LA_{LLF} is the LLF area. Illumination of the SLF area was obtained by shading the margin of the previously illuminated LLF area with a template as described before. Stomatal conductance of the SLF area (previously illuminated with the LLF) could not be measured so that conductance of the SLF was assumed to be similar to that of the LLF (g_{LLF}). Therefore, g_{LLF} was taken as an approximation of stomatal conductance for CO_2 (g_c) of the LLF and SLF areas.

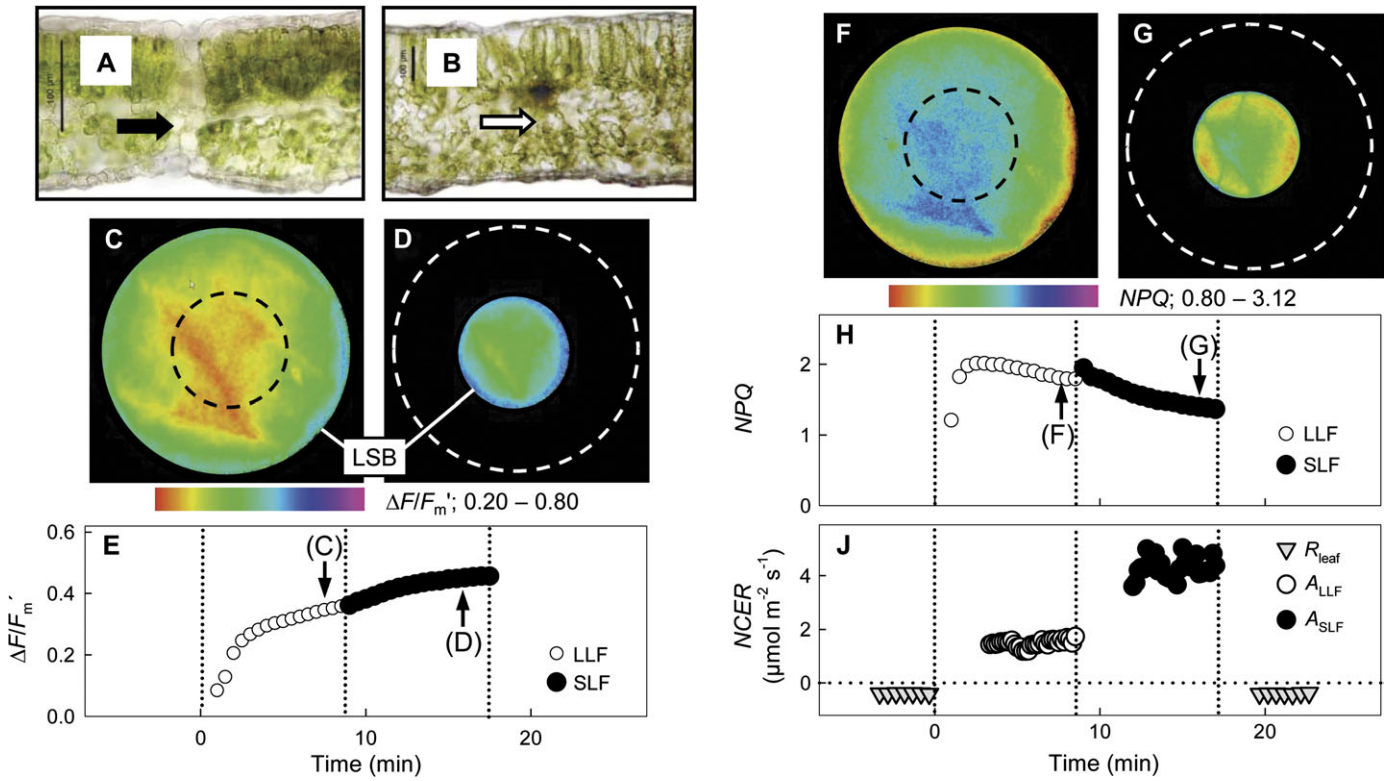

Fig. 1. Transverse sections of (A) a heterobaric leaf of *Glycine max* where the bundle sheath extension (black arrow) completely separates the intercellular spaces of adjacent areoles and (B) a homobaric leaf of *Vicia faba* where no bundle sheath extensions are visible (white arrow; scale bars: 100 μm). Chlorophyll fluorescence and gas exchange of a *V. faba* leaf measured under photorespiratory conditions and illuminated either with a large (LLF with a diameter of 23 mm; C, F) or a small (SLF with a diameter of 10 mm; D, G) lightfleck. Images of $\Delta F/F_m'$ when (C) the LLF area (black dashed line indicates the central area subsequently illuminated by the SLF) and (D) the SLF area (white dashed line indicates the previous LLF position) were illuminated. (C) The averaged $\Delta F/F_m'$ values of the LLF area (open symbols) and the SLF area (closed symbols) versus time after illumination had started; the arrows denote the times the images (C, D) were taken. Images of *NPQ* when (F) the LLF area and (G) the SLF area were illuminated. (H) Averaged *NPQ* values of the LLF area and the SLF area; the arrows denote the times the images (F, G) were taken. (J) Net CO_2 exchange rates (*NCER*) of the leaf measured in the dark (R_{leaf}; PPFD ~1–3 μmol photons m^{-2} s^{-1}) and of the LLF (A_{LLF}) and SLF areas (A_{SLF}) in the light (150 μmol m^{-2} s^{-1}). Due to applied drought stress, stomatal conductance (g_c) was low (16.1±1.1 mmol CO_2 m^{-2} s^{-1}).

Whole leaf *NCER* was denoted $NCER_{leaf}$, with negative values indicating dark respiration (R_{leaf}=–*NCER*) and positive values indicating the net CO_2 assimilation rate (A; Fig. 1J). $NCER_{leaf}$ measured with LLF or SLF illumination was denoted $NCER_{leaf,LLF}$ and $NCER_{leaf,SLF}$, respectively. The gross assimilation rate (A^*) of the LLF leaf area was calculated as:

$$A^*_{LLF} = (NCER_{leaf,LLF} - R_{leaf}) \frac{LA_{leaf}}{LA_{LLF}} \quad (2)$$

and for the SLF area as:

$$A^*_{SLF} = (NCER_{leaf,SLF} - R_{leaf}) \frac{LA_{leaf}}{LA_{SLF}}. \quad (3)$$

The assimilation rates of the LLF and SLF leaf areas were then calculated as $A_{LLF}=A^*_{LLF}+R_{leaf}$ and $A_{SLF}=A^*_{SLF}+R_{leaf}$, respectively.

The electron requirement for assimilated CO_2 (ETR/A^*) was calculated for the LLF (ETR_{LLF}/A^*_{LLF}) and the SLF (ETR_{SLF}/A^*_{SLF}). Regression analysis of the ETR/A^* ratio (Fig. 5) and the data shown in Fig. 3E, F was performed with Table Curve (SPSS Inc.) by using least squares analysis. For linear and inverse linear regression analyses, the software SigmaPlot (SPSS Inc.) was used. *T*-tests were applied to analyse the data shown in Fig. 4 with the null hypothesis that the coefficient of the independent variable is zero with statistically significant differences for $P < 0.05$ (Table 1). Further data analysis was performed with a simplified geometrical model which combines photosynthetic CO_2 uptake of the different lightflecks.

Simplified model of geometric dependence of CO_2 uptake of the lightflecks

Lateral CO_2 diffusion from shaded areas may affect A, $\Delta F/F_m'$, and *NPQ* of illuminated parts of homobaric leaves. For simplicity, only A is treated in the model. A_{LLF} and A_{SLF} denote the average assimilation rates of the LLF and SLF areas (Fig. 1), respectively. The geometrical dependency of assimilation can be quantified by the ratio A_{LLF}/A_{SLF} as a function of g_c. For both the LLF and SLF areas, assimilation rates can be considered to be composed of two regions: (i) the assimilation rate of an outer region (A_{lat}) which is adjacent to the shade and affected by lateral CO_2 supply from the shaded areas in addition to vertical CO_2 supply through the stomata; and (ii) the assimilation of an inner lightfleck region (A_{st}) only depending on CO_2 supply through the stomata (Figs. 6 and 2). This classification is sustainable as long as the lateral diffusion distance of CO_2 (Δr) across the light–shade border is small compared with the radius of the LLF or SLF (R or r). The average A_{LLF} of the LLF area with the radius R is given by:

Table 1. Estimated regression parameters a, b, a′, and b′ as function of stomatal CO_2 conductance (g_c) under photorespiratory and non-photorespiratory conditions

Regression equation	Physiological parameter	[O_2] (%)	*Vicia faba* (homobaric) a	b	*Glycine max* (heterobaric) a	b
$f(g_c)=ag_c+b$	A_{LLF}	21	0.07±0.01*	0.53±0.20*	0.08±0.01*	0.26±0.58
		1	0.11±0.01*	0.77±0.59	0.11±0.02*	–0.52±0.81
	A_{SLF}	21	0.07±0.01*	3.09±0.31*	0.09±0.02*	0.79±0.71
		1	0.11±0.02*	3.74±0.70*	0.13±0.02*	–0.57±0.94
			a′	**b′**	**a′**	**b′**
$f(g_c)=a'g_c^{-1}+b'$	$A_{LLF/SLF}$	21	–4.53±0.78*	0.76±0.05*	–0.10±0.77	0.83±0.03*
		1	–3.99±0.85*	0.68±0.05*	0.02±0.70	0.86±0.03*
	$\Delta F/F_m'_{LLF/SLF}$	21	–4.02±0.73*	0.90±0.05*	0.10±0.58	0.92±0.03*
		1	–1.79±0.61*	0.96±0.03*	0.36±0.80	0.90±0.04*
	$NPQ_{LLF/SLF}$	21	7.68±1.47*	0.83±0.09*	–0.49±1.06	0.96±0.05*
		1	2.10±1.80	1.21±0.11*	–1.85±0.88*	0.98±0.04*

Mean values of the regression parameters (±SEM) were obtained from the denoted regression equations by fitting the respective data of Fig. 3 (parameter a and b; linear fit) and Fig. 4 (parameter a′ and b′; for a simplified geometric model see Materials and methods).
Asterisks indicate values significantly different from 0 (a, b, and a′) or 1 (b′) (P <0.05).

$$A_{LLF}=\frac{A_{st}\pi(R-\Delta r)^2+A_{lat}\pi\left(R^2-(R-\Delta r)^2\right)}{\pi R^2} \quad (4)$$

A short calculation renders:

$$A_{LLF}=(A_{st}-A_{lat})\frac{(R-\Delta r)^2}{R^2}+A_{lat}. \quad (5)$$

Because Δr is small compared with R, we can approximate:

$$\frac{(R-\Delta r)^2}{R^2}=\frac{R^2-2\Delta rR+\Delta r^2}{R^2}\approx 1-2\frac{\Delta r}{R}. \quad (6)$$

Thus, A_{LLF} can be approximated by the term:

$$A_{LLF}=A_{st}+2(A_{lat}-A_{st})\frac{\Delta r}{R}. \quad (7)$$

A similar expression is found for the average assimilation rate of the small lightfleck, A_{SLF} (substitution of R by r). Thus, the LLF to SLF ratio is:

$$\frac{A_{LLF}}{A_{SLF}}=\frac{A_{st}+2(A_{lat}-A_{st})\Delta r/R}{A_{st}+2(A_{lat}-A_{st})\Delta r/r}. \quad (8)$$

Moreover, because Δr is small compared with r, the geometric series can be used to approximate the ratio:

$$\frac{A_{LLF}}{A_{SLF}}\approx 1-\frac{(A_{lat}-A_{st})}{A_{st}}\left(\frac{2}{r}-\frac{2}{R}\right)\Delta r. \quad (9)$$

The functional dependence of Δr on g_c is not concrete in the sense that it depends on actual definition of Δr (diffusion is a continuous process). However, Δr becomes monotonically small, eventually zero for large g_c. Several empirical functions could therefore be used (exponential, rational, etc.). Here, a very simple function has been used:

$$\Delta r=\frac{\alpha}{g_c} \quad (10)$$

where α is a positive constant. Finally, a possible model to fit the ratios is then:

$$\frac{A_{LLF}}{A_{SLF}}=\frac{a'}{g_c^{-1}}+b' \quad (11)$$

where:

$$a'=-\alpha\frac{A_{lat}-A_{st}}{A_{st}}\left(\frac{2}{r}-\frac{2}{R}\right) \quad (12)$$

is a negative constant. Inspection of a' reveals that it is composed of three parts: the first, α, contains the sensibility of Δr towards changes in g_c; the second, $(A_{lat}–A_{st})/A_{st}$, describes implicitly the dependence on the lateral diffusivity of the leaf; the third, $(2/r–2/R)$, models the geometric aspect. In general a' is expected to approach 0 when there is no lateral CO_2 supply or to differ substantially from 0 when LLA and SLA are influenced by lateral CO_2 diffusion. The parameter b' of Equation 11 is a saturation value which ideally has a value of 1 when g_c is high; that is, the stomata are fully open. The model was used to calculate the parameters a′ and b′ summarized in Table 1 by fitting the LLF/SLF ratios of various physiological parameters shown in Fig. 4.

Results

The maximum quantum yield (F_v/F_m) of dark-adapted leaves was 0.80±0.02 (n=44) for leaves of *G. max* (heterobaric leaf anatomy, Fig. 1A) and 0.78±0.02 (n=47) for *V. faba* (homobaric leaf anatomy, Fig. 1B), indicating that photosynthesis was not photoinhibited under the imposed drought stress. When homobaric *V. faba* leaves were illuminated by large (LLF) or small lightflecks (SLF), the quantum yield of light-adapted leaves ($\Delta F/F_m'$) was highest near the light–shade borders (Fig. 1C, D) for plants under drought stress with low stomatal conductance (g_c) (16.1±1.1 mmol CO_2 m^{-2} s^{-1}). For the LLF (Fig. 1C) the averaged $\Delta F/F_m'$ value was lower when that area was illuminated by the SLF (Fig. 1D, E). The opposite was found for non-photochemical quenching (NPQ) as a measure of heat dissipation, with lowest values near the light–shade borders (Fig. 1F, G), while the averaged NPQ value of the LLF was higher than that of the SLF area (Fig. 1H). Simultaneous measurement of net CO_2 exchange rates (NCERs) showed respiration rates (R_{leaf}=–$NCER_{leaf}$) of 0.39±0.02 μmol m^{-2} s^{-1} when the leaf was in darkness, net

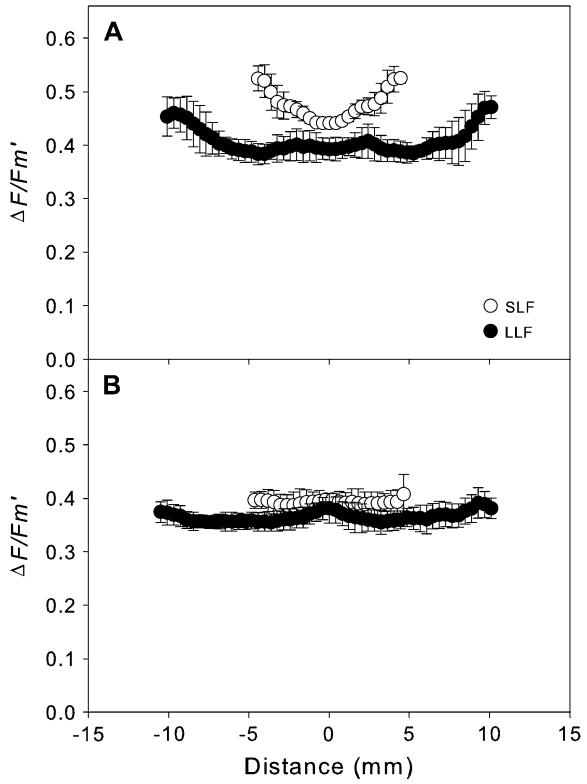

Fig. 2. Radial gradients of $\Delta F/F_m'$ values of SLF (open symbols) and LLF (closed symbols) areas of leaves of (A) *Vicia faba* measured at a stomatal conductance of (g_c) 16.1±1.1 mmol CO_2 m^{-2} s^{-1}; (B) *Glycine max* measured at a g_c of 12.4±0.7 mmol CO_2 m^{-2} s^{-1}. The error bars indicate the standard deviation obtained from six $\Delta F/F_m'$ gradients on each lightfleck.

CO_2 assimilation rates of the LLF area (A_{LLF}) of 1.48±0.13 μmol m^{-2} s^{-1}, and 4.28±0.37 μmol m^{-2} s^{-1} for the SLF area (A_{SLF}; Fig. 1J). Comparing the perimeter to area ratios of the LLF and SLF resulted in a factor of 0.43, while the A_{LLF} to A_{SLF} ratios showed a factor of 0.34 (Fig. 1J). However, this can vary between 0.7 and 0.2 as shown in Fig. 4A.

Radial profiles of $\Delta F/F_m'$ of the SLF and LLF areas showed large differences between *V. faba* and *G. max* (Fig. 2). The $\Delta F/F_m'$ values for *V. faba* were higher at the edges than in the centre of the profiles and larger for the SLF than the LLF (Fig. 2A). For *G. max*, however, the $\Delta F/F_m'$ profiles showed only small differences between the centres and the edges, and between SLF and LLF areas (Fig. 2B).

For homobaric *V. faba* leaves, A_{SLF} was larger than A_{LLF} at all g_c values (Fig. 3A), but this was not the case for heterobaric *G. max* leaves (Fig. 3B). Linear regression of A_{LLF} and A_{SLF} versus g_c of *V. faba* and *G. max* leaves resulted in similar slopes of 0.07–0.09 under photorespiratory conditions (21% [O_2]) and of 0.11–0.13 under non-photorespiratory conditions (1% [O_2]; Table 1). For *V. faba*, the axis intercepts of A_{SLF} were significantly larger than zero and substantially larger than A_{LLF}. For *G. max*, the intercepts were not significantly different from zero independently of LLF or SLF illumination (Table 1). For both homobaric and heterobaric leaves, the $\Delta F/F_m'$ values declined with decreasing g_c values. The slope was smaller for the SLF than the LLF areas of homobaric *V. faba* leaves (Fig. 3C), whereas no differences between SLF and LLF were observed for heterobaric *G. max* leaves (Fig. 2D). In contrast, *NPQ* increased with decreasing g_c (Fig. 3E, F), with a smaller slope for the SLF than the LLF areas for *V. faba* (Fig. 3E) but no differences for *G. max* (Fig. 3F).

Differences between measured gas exchange and chlorophyll fluorescence parameters of the LLF and SLF areas were evaluated by analysing the dependence of the LLF/SLF ratios of net CO_2 assimilation rates, quantum yield, and non-photochemical quenching on g_c with inverse linear regression (ratio=b′+a′/g_c) (Fig. 4 and Table 1). The ratios denoted $A_{LLF/SLF}$, $\Delta F/F_m'_{LLF/SLF}$, and $NPQ_{LLF/SLF}$ showed substantial differences between homobaric and heterobaric leaves. For *V. faba*, the inverse linear regression parameters a′ were significantly different from zero for all ratios (except $NPQ_{LLF/SLF}$ obtained under 1% [O_2]), whereas for *G. max* the a′ values were not different from zero apart from $NPQ_{LLF/SLF}$ measured at 1% [O_2]. The saturation value b' ranged between 0.68 and 1.21 for both species.

Ratios between the ETR and gross assimilation rate (A^*) were calculated from data of combined gas exchange and chlorophyll fluorescence measurements. For LLF areas of *V. faba* leaves, ETR/A^* values were up to 25 at low and ~6 at high g_c under 21% [O_2], and ~6 at low and 3 at high g_c under 1% [O_2] (Fig. 5A). For the SLF areas, ETR/A^* was only slightly affected by g_c under both 21% and 1% [O_2] (Fig. 5B). For *G. max* leaves, the ETR/A^* ratios were very similar for both the LLF and SLF areas, with values up to 20 at low (<30 mmol m^{-2} s^{-1}) and ~6 at high g_c under 21% [O_2] and up to 8 at low and 2–3 at high g_c with 1% [O_2] (data not shown).

Discussion

Photosynthesis is progressively impeded during drought stress mainly because of decreasing stomatal conductance, and the photosynthetic response can be understood as direct adjustment of the metabolism to low CO_2 availability (Flexas *et al.*, 2004). Decreasing CO_2 availability due to stomatal closure was, in part, compensated in homobaric *V. faba* leaves by lateral CO_2 diffusion from shaded to illuminated leaf parts, as indicated by an increase in *A* and $\Delta F/F_m'$ and a decrease in *NPQ* resulting in higher carbon gain and lower light stress in the small rather than the large lightfleck areas (LLF/SLF ratios <1; Fig. 4). In heterobaric *G. max* leaves, lateral CO_2 diffusion was not effective in either LLF or SLF areas.

Since lateral CO_2 diffusion increased CO_2 uptake while the rate of transpiration or stomatal conductance was not influenced (data not shown), the efficiency of water use also increased as previously reported (Morison *et al.*, 2007; Pieruschka *et al.*, 2008). However, the measurements of transpiration and stomatal conductance bear some uncertainties when measuring water fluxes of entire leaves which are partly shaded. Therefore, more detailed studies are necessary to quantify this effect.

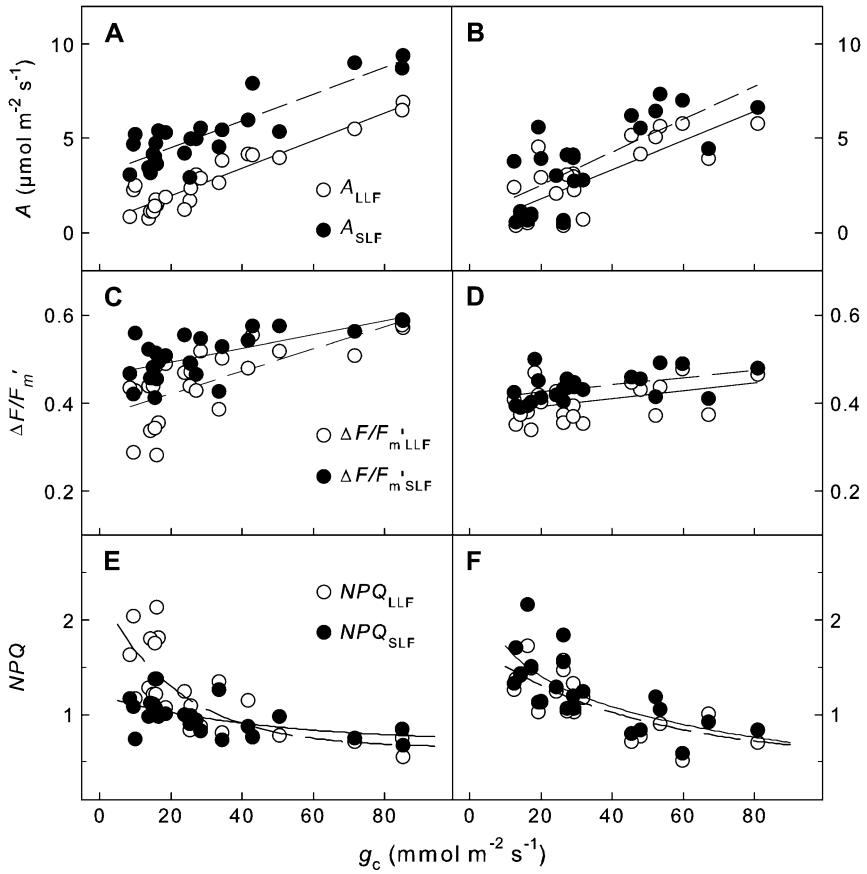

Fig. 3. (A and B) Net CO_2 assimilation rates (*A*), (C and D) effective quantum yield of PSII ($\Delta F/F_m'$), and (E and F) non-photochemical quenching (*NPQ*) as a function of stomatal conductance (g_c) of homobaric *V. faba* (A, C, E) and heterobaric *G. max* leaves (B, D, F) illuminated with an LLF and, subsequently, an SLF. The plants were exposed to different drought levels with 1–5 d without irrigation. The experiments were performed under photorespiratory conditions (21% [O_2]); regression analysis was performed by least squares analysis.

Following illumination, thermal dissipation can be activated rapidly by de-epoxidation of xanthophylls, a mechanism very sensitive to changes in light intensity (Watling *et al.*, 1997). The impact of CO_2 re-fixation is particularly large for drought-stressed plants with low g_c where lateral CO_2 flux may be the major source of CO_2, especially for SLF areas. For example, while A_{LLF} of *V. faba* reached values of ~0 μmol CO_2 m^{-2} s^{-1} at low stomatal conductance, A_{SLF} was still substantially higher under these conditions (Fig. 3A). The *ETR* depends on c_i, and the rate of CO_2 assimilation and stomatal conductance may be driven by the *ETR* (Weis and Berry, 1987; Genty *et al.*, 1989). An increase in *ETR*/*A** (Fig. 5) is regarded as an indicator for stomatal limitations paralleled by an increase in alternative pathways of electron flow such as photorespiration (Cornic and Fresneau, 2002; Flexas and Medrano, 2002; Kitao *et al.*, 2003; Bota *et al.*, 2004). When heterobaric *G. max* leaves were illuminated with LLF or SLF, the *ETR*/*A** ratios were not different (data not shown). For homobaric *V. faba* leaves, the *ETR*/*A** values were substantially smaller in the SLF than the LLF areas due to CO_2 delivered from shaded leaf parts largely reducing stomatal limitations on photosynthesis (Fig. 5).

The LLF to SLF ratios as a function of stomatal conductance are described by a geometrical model which considers the dependency of a circular area on its radius (see Materials and methods). The ratio of the perimeter to area ratio of LLF (4 cm^{-1}) and SLF (1.7 cm^{-1}) is 0.43 and, when, for example, the ratios of the assimilation rates ($A_{LLF/SLF}$) would follow the lightfleck geometry the lower limit of $A_{LLF/SLF}$ would approach 0.43. However, $A_{LLF/SLF}$ was found to be substantially lower (Fig. 4A). If a lightfleck is influenced by lateral CO_2 then, as shown in Figs. 2 and 6, some portion of this lightfleck along the light–shade border (Δr) has a higher quantum yield and rate of assimilation (A_{lat}) then the centre of the lightfleck (A_{st}). The average assimilation of the LLF or SLF is therefore determined by the Δr, which is additionally affected by the non-linear response of photosynthesis to CO_2. The resulting $A_{LLF/SLF}$ or $\Delta F/F_m'_{LLF/SLF}$ may differ from geometrical constraints.

Re-fixation of remotely supplied CO_2 additionally depends on a range of parameters and conditions. Leaves in different layers of a canopy are exposed to sunflecks with varying intensities, and duration ranging between seconds and minutes (Pfitsch and Pearcy, 1989; Pearcy *et al.*, 1994). The differences in light intensity of the illuminated and

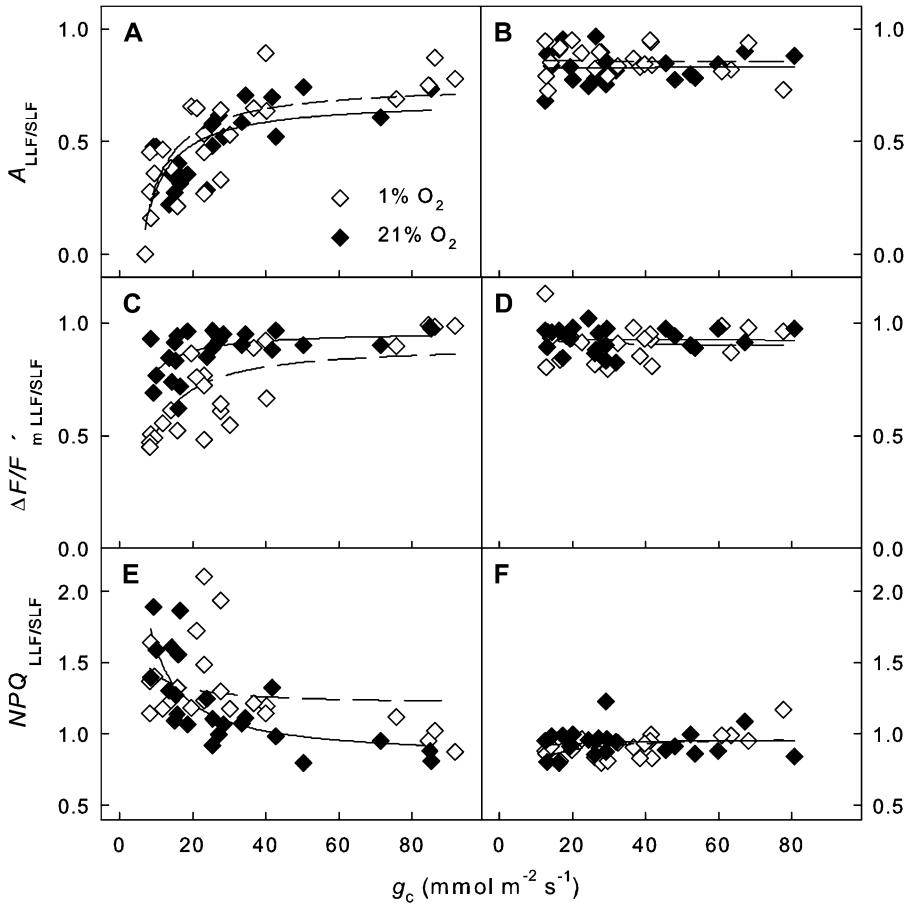

Fig. 4. Ratios of the LLF to SLF areas versus stomatal conductance (g_c). (A and B) Ratios of assimilation rates ($A_{LLF/SLF}$), (C and D) effective quantum yield of PSII ($\Delta F/F_m'_{LLF/LLF}$), and (E and F) non-photochemical quenching ($NPQ_{LLF/SLF}$) of *V. faba* (A, C, E) and *G. max* (B, D, F) leaves under photorespiratory (21% [O_2]) and non-photorespiratory (1% [O_2]) conditions. The data were fitted by using a simplified model considering lightfleck geometries (see Materials and methods), and the calculated parameters a' and b' are summarized in Table 1.

shaded leaf areas as well as stomatal conductance may greatly influence lateral gradients in c_i. Additionally the shape, size, and interconnectivity of intercellular gas spaces can be very variable, for example between plant species or even leaves of the same plant (Neger, 1918; Wylie, 1952; Jahnke and Krewitt, 2002; Pieruschka *et al.*, 2005), and affect lateral CO_2 diffusivity which can reach values up to 40% of diffusion in free air (Pieruschka *et al.*, 2005). Stomatal conductance largely determines the ratio of the supply of photosynthesis by lateral CO_2 diffusion inside the leaf and 'vertical' CO_2 diffusion from the external air through the stomata (Pieruschka *et al.*, 2008). Finally, a non-linear response of photosynthesis may additionally influence the re-fixation of laterally delivered CO_2 and under Rubisco-limited conditions the response may be larger than under RubP-limited conditions (von Caemmerer, 2000).

Stomatal response to rapidly fluctuating light conditions may be rather slow, in particular under drought stress, and leaf internal c_i gradients may be very variable in dynamically fluctuating conditions. For example, when a sunfleck emerges on a leaf with an activated photosynthetic apparatus, c_i is likely to decrease quickly, resulting in a large lateral Δc_i between shaded and illuminated areas. A gradual increase of stomatal conductance with the duration of the sunfleck exposure would then increase the vertical CO_2 supply from ambient air through the stomata, and the lateral Δc_i would decrease. Thus, leaf internal CO_2 concentration in sunfleck areas may be extremely variable, and detection of such fast and dynamic processes is very difficult with conventional measuring techniques. The response of stomatal conductance of drought-stressed plants may be slow and reduced as compared with well-watered plants. Thus, lateral CO_2 diffusion could support photosynthesis during transient opening of stomata more effectively, in particular in a dynamic light environment under drought stress. The present study confirms previous results with drought-stressed *V. faba* and *N. tabacum* plants where lateral CO_2 diffusion from shaded leaf parts affected $\Delta F/F_m'$ and *NPQ* in adjacent illuminated areas up to 4 mm from a light–shade border, as measured with chlorophyll fluorescence imaging (Pieruschka *et al.*, 2006). Studies in which stomata were closed with grease also came to the general conclusion that lateral CO_2 flux may support photosynthesis and, although greasing of stomata is an

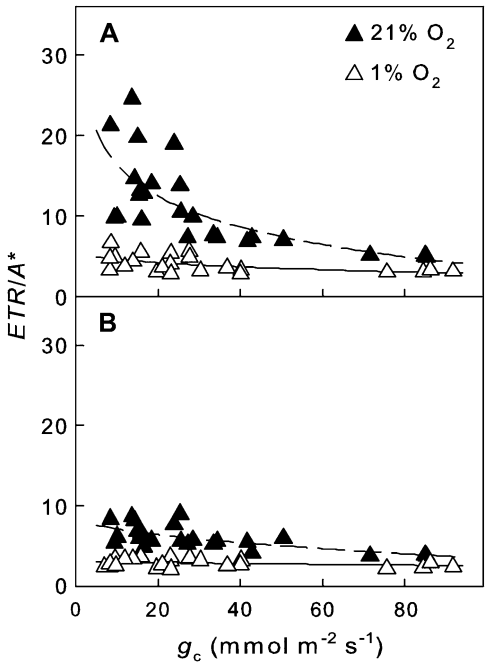

Fig. 5. Electrons required for assimilated CO_2 (*ETR/A**) of homobaric leaves of *V. faba* illuminated by (A) an LLF or (B) an SLF. The experiments were performed under photorespiratory (closed symbols, dashed regression lines) and non-photorespiratory conditions (open symbols, solid regression lines).

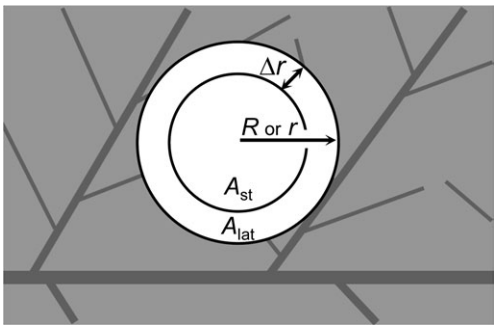

Fig. 6. Scheme of a lightfleck illustrating parameters used for the simplified model calculation (see Equation 6). R is the radius of the large light fleck (LLF) and r of the small light fleck (SLF). A_{st} is the averaged net CO_2 assimilation rate of the denoted inner area of the respective lightflecks (LLF or SLF) where CO_2 supply is only through stomata; A_{lat} is the averaged net CO_2 assimilation rate of the outer area of the respective lightflecks with an additional lateral CO_2 supply from adjacent areas. Δr designates the effective diffusion distance of CO_2 into the lightfleck.

artificial treatment, it has proved to be very useful in estimating leaf internal diffusivities (Duarte *et al.*, 2005; Morison *et al.*, 2007; Pieruschka *et al.*, 2008).

What the function is of homobaric leaves in natural ecosystems and whether lateral diffusion inside such leaves is effective in efficient carbon gain or water use is an intriguing question. Rainforest understorey and subcanopy species were reported to have homobaric leaves while light-exposed species are characterized by heterobaric leaves (Kenzo *et al.*, 2007). This observation may correlate with the fact that only the upper layers of plant canopies are exposed to saturating light whereas leaves in the shaded layers obtain light mainly from sunflecks (up to 90% of daily photon flux; Pfitsch and Pearcy, 1989). Plants exposed to a fluctuating light environment as in forest understorey may thus benefit from having homobaric leaves which are capable of utilizing laterally supplied CO_2. This effect is obviously dependent on stomatal conductance and usually shade leaves open their stomata rather slowly after exposure to light when compared with sun leaves; however, once the stomata are fully open the closing mechanism is also very slow when the leaves are exposed to darkness again (Ooba and Takahashi, 2003). However, most of these experiments were performed by illuminating entire leaves or at least homogenously illuminated leaf areas inside leaf chambers. Whether stomata respond in the same way when only a small leaf area is illuminated or when a lightfleck is moving over the leaf blade while the other leaf part is exposed to shade is not known. This question is rather important to understand the productivity of understorey plants and their contribution to the overall carbon fluxes, and further studies and new methods to elucidate this effect are necessary.

In conclusion, lateral diffusion of CO_2 was found to contribute to photosynthesis of lightfleck areas of homobaric leaves and the contribution increases with smaller lightflecks. Additionally, lateral CO_2 diffusion reduces the light stress and most probably increases the water use efficiency. Stomatal conductance is the key player which determines the amount of lateral CO_2 supply to lightflecks. When stomatal conductance is high then the importance of lateral CO_2 diffusion for lightfleck photosynthesis is small, but it becomes substantial when stomata are closed.

Acknowledgements

We are indebted to Dr Shizue Matsubara for critical reading of the manuscript. This work was part of the doctoral thesis of RP at Mathematisch-Naturwissenschaftliche Fakultät, Heinrich-Heine Universität, Düsseldorf, Germany.

References

Bilger W, Björkman O. 1990. Role of the xanthophyll cycle in photoprotection elucidated by measurements of light-induced absorbance changes, fluorescence and photosynthesis in leaves of *Hedera canariensis*. *Photosynthesis Research* **25,** 173–185.

Bota J, Medrano H, Flexas J. 2004. Is photosynthesis limited by decreased Rubisco activity and RuBP content under progressive water stress? *New Phytologist* **162,** 671–681.

Cornic G, Fresneau C. 2002. Photosynthetic carbon reduction and carbon oxidation cycles are the main electron sinks for photosystem II activity during a mild drought. *Annals of Botany* **89,** 887–894.

Duarte HM, Jakovljevic I, Kaiser F, Lüttge U. 2005. Lateral diffusion of CO_2 in leaves of the crassulacean acid metabolism plant *Kalanchoe daigremontiana* Hamet et Perrier. *Planta* **220,** 809–816.

Flexas J, Bota J, Loreto F, Cornic G, Sharkey TD. 2004. Diffusive and metabolic limitations to photosynthesis under drought and salinity in C_3 plants. *Plant Biology* **6,** 269–279.

Flexas J, Medrano H. 2002. Drought-inhibition of photosynthesis in C_3 plants: stomatal and non-stomatal limitations revisited. *Annals of Botany* **89,** 183–189.

Genty B, Briantais JM, Baker NR. 1989. The relationship between the quantum yield of photosynthetic electron transport and quenching of chlorophyll fluorescence. *Biochimica et Biophysica Acta* **990,** 87–92.

Hetherington AM, Woodward FI. 2003. The role of stomata in sensing and driving environmental change. *Nature* **424,** 901–908.

Jahnke S. 2001. Atmospheric CO_2 concentration does not directly affect leaf respiration in bean or poplar. *Plant, Cell and Environment* **24,** 1139–1151.

Jahnke S, Krewitt M. 2002. Atmospheric CO_2 concentration may directly affect leaf respiration measurement in tobacco, but not respiration itself. *Plant, Cell and Environment* **25,** 641–651.

Kenzo T, Ichie T, Watanabe Y, Hiromi T. 2007. Ecological distribution of homobaric and heterobaric leaves in tree species of Malaysian lowland tropical rainforest. *American Journal of Botany* **94,** 764–775.

Kitao M, Lei TT, Koike T, Tobita H, Maruyama Y. 2003. Higher electron transport rate observed at low intercellular CO_2 concentration in long-term drought-acclimated leaves of Japanese mountain birch (*Betula ermanii*). *Physiologia Plantarum* **118,** 406–413.

Loreto F, Velikova V, Di Marco G. 2001. Respiration in the light measured by $^{12}CO_2$ emission in $^{13}CO_2$ atmosphere in maize leaves. *Australian Journal of Plant Physiology* **28,** 1103–1108.

Morison JIL, Gallouet E, Lawson T, Cornic G, Herbin R, Baker NR. 2005. Lateral diffusion of CO_2 in leaves is not sufficient to support photosynthesis. *Plant Physiology* **139,** 254–266.

Morison JIL, Lawson T, Cornic G. 2007. Lateral CO_2 diffusion inside dicotyledonous leaves can be substantial: quantification in different light intensities. *Plant Physiology* **145,** 680–690.

Neger F. 1918. Wegsamkeit der Laubblätter für Gase. *Flora* **111,** 152–161.

Ooba M, Takahashi H. 2003. Effect of asymmetric stomatal response on gas-exchange dynamics. *Ecological Modelling* **164,** 65–82.

Pearcy RW, Chazdon RL, Gross LJ, Mott KA. 1994. Photosynthetic utilisation of sunfleck: a temporarily patchy resource on a time scale of seconds to minutes. In: Caldwell MM, Pearcy RW, eds. *Exploitation of environmental heterogeneity by plants*. San Diego: Academic Press, 175–208.

Pfitsch WA, Pearcy RW. 1989. Daily carbon gain by *Adenocaulon bicolor* (Asteraceae), a redwood understory forest herb, in relation to its light environment. *Oecologia* **80,** 465–470.

Pieruschka R, Chavarria-Krauser A, Cloos K, Scharr H, Schurr U, Jahnke S. 2008. Photosynthesis can be enhanced by lateral CO_2 diffusion inside leaves over distances of several millimeters. *New Phytologist* **178,** 335–347.

Pieruschka R, Schurr U, Jahnke S. 2005. Lateral gas diffusion inside leaves. *Journal of Experimental Botany* **56,** 857–864.

Pieruschka R, Schurr U, Jensen M, Wolff WF, Jahnke S. 2006. Lateral diffusion of CO_2 from shaded to illuminated leaf parts affects photosynthesis inside homobaric leaves. *New Phytologist* **169,** 788.

Pinelli P, Loreto F. 2003. $^{12}CO_2$ emission from different metabolic pathways measured in illuminated and darkened C_3 and C_4 leaves at low, atmospheric and elevated CO_2 concentration. *Journal of Experimental Botany* **54,** 1761–1769.

von Caemmerer S. 2000. *Biochemical models of photosynthesis*. Victoria, Australia: Commonwelth Scientific and Industrial Research Organisation Publications.

von Caemmerer S, Farquhar GD. 1981. Some relation between the biochemistry of photosynthesis and the gas exchange of leaves. *Planta* **153,** 376–387.

Watling JR, Robinson SA, Woodrow IE, Osmond CB. 1997. Responses of rainforest understorey plants to excess light during sunflecks. *Australian Journal of Plant Physiology* **24,** 17–25.

Weis E, Berry JA. 1987. Quantum efficiency of photosystem II in relation to 'energy'-dependent quenching of chlorophyll fluorescence. *Biochimica et Biophysica Acta* **894,** 198–208.

Wylie RB. 1952. The bundle sheath extension in leaves of dicotyledons. *American Journal of Botany* **39,** 645–651.